

4-1-2023

Piperazine-Based Metallopolymers for Bioengineering Applications

Jessica K. Schneider
University of Dayton

Follow this and additional works at: https://ecommons.udayton.edu/uhp_theses

eCommons Citation

Schneider, Jessica K., "Piperazine-Based Metallopolymers for Bioengineering Applications" (2023).
Honors Theses. 425.
https://ecommons.udayton.edu/uhp_theses/425

This Honors Thesis is brought to you for free and open access by the University Honors Program at eCommons. It has been accepted for inclusion in Honors Theses by an authorized administrator of eCommons. For more information, please contact mschlangen1@udayton.edu, ecommons@udayton.edu.

Piperazine-Based Metallopolymers for Bioengineering Applications



Honors Thesis

Jessica Schneider

Department: Chemistry

Advisors: Justin Biffinger, Ph.D. and Russell K. Pirlo, Ph.D.

April 2023

Piperazine-Based Metallopolymers for Bioengineering Applications

Honors Thesis

Jessica Schneider

Department: Chemistry

Advisors: Justin Biffinger, Ph.D. and Russell K. Pirlo, Ph.D.

April 2023

Abstract

Engineering realistic and functional tissue models presents promising possibilities in drug discovery and other biomedical research. A novel polymer with potential applications in biomedical studies was developed. I report the first synthesis and characterization (with NMR, IR, GPC, UV-vis spectroscopy, and thermal analysis) of two thermoplastic poly(alkyl piperazine succinate) diols with either propyl or hexyl alkane chains bridging the piperazines. These polyester diols were chain extended with hexamethylene diisocyanate to create highly amorphous polyester urethane thermoplastic polymers. Ru(III) and Fe(III) was then successfully coordinated with these polymers, producing a total of four different metallopolymers. The crosslinking of these complexes introduces degradative properties to the polymer, which could be valuable in biomedical studies.

Acknowledgements

I would like to acknowledge all the individuals and programs that have provided the mentorship and funding necessary for the completion of this project. This research was financially supported by the ISE Summer CoRPs Fellowship, the College of Arts and Sciences Dean's Summer Fellowship, and the Honors Program. The ISE Summer CoRPs and the Dean's Summer Fellowship allowed me to discover my research interests while also growing professionally and making friends along the way. My mentors, Dr. Biffinger and Dr. Pirlo, ensured my success by continuously providing their support and guidance not only throughout this project, but throughout my undergraduate career. The skills I learned while under their guidance will stick with me for the rest of my life. I would also like to thank my professors, friends, and family for their constant support and belief in me and my dreams.



University of
Dayton

Table of Contents

Abstract	Title Page
Introduction	5
Methodology	7
Results and Data Analysis	14
Discussion and Conclusion	32

Table of Reaction Schemes

Scheme 1 Structures of 3,3'-(piperazine-1,4-bis(propan-1-ol)) and 6,6'-(piperazine-1,4-bis(hexan-1-ol))	9
Scheme 2 Polymerization of compounds 1 or 2 with dimethyl succinate	10
Scheme 3 Chain extension of PPPS-OL or PHPS-OL with hexamethylene diisocyanate	11
Scheme 4 Metalation of chain extended Poly(piperazine succinate) diols with either Fe(III) or Ru(III)	13

Table of Figures

Figure 1 Binding modes for piperazine in the chair (1) and boat (2) conformations	6
Figure 2 ¹ H NMR data for (A) PPPS-OL and (B) PHPS-OL	17
Figure 3 Infrared spectroscopy results for polymers before and after chain extension	21
Figure 4 GPC comparisons of polymers before and after chain extension	22

Figure 5 DSC traces of heating from -10 °C to 170 °C (A) PPPS-C and (B) PHPS-C at 10 °C /min and the cooling from 170 °C to -10 °C (C) PPPS-C and (D) PHPS-C at 10 °C /min with and without Ru(III) or Fe(III)	24
Figure 6 UV-visible spectroscopy data for non-metal and metal-containing polymers	26
Figure 7 GPC data for non-metal and metal-containing polymers	27
Figure 8 Comparison of hydrolysis for non-metal and metal-containing polymers	31
Figure 9 Scanning electron microscope images for PLA/PHPS fibers	32

Table of Tables

Table 1 Summary of the molecular weights of the major products from the chain extended polypiperazine polymers and Ru(III) and Fe(III) metallopolymers.	18
--	----

1 | Introduction

Metal coordination polymers (or metallopolymers) represent a continuously expanding domain of material science with a wide array of potential applications¹, ranging from memory and data storage² to biomedical sensors³ and cancer therapies⁴. This diversity of applications can be accredited to the ability of ligands to coordinate with metals in the polymer backbone and the manipulation of the metal redox potentials. Metal coordination in the polymers can create extended networks of immobilized metal centers, allowing control of the physical properties of the polymeric material⁵. The choice of ligand therefore permits the creation of unique molecular scaffolding materials and presents a wide array of research opportunities.

Alkylated piperazines are versatile polymer structural components since they contain tertiary nitrogen binding sites that can bind metal centers in a bidentate configuration from the boat conformation, or monodentate from the chair conformation⁶. Binding of metals from the most stable chair conformation could allow for two different metal ions to be coordinated by one piperazine, allowing crosslinking between polymer chains through several different binding modes based on the metal oxidation state or size of the metal ionic radius. The binding modes are visualized in **Figure 1**. The piperazine scaffold has been used in the development of many commercially available drugs⁷ and within metal organic frameworks (MOFs). MOFs have many applications in drug delivery⁸ and ion exchange⁹.

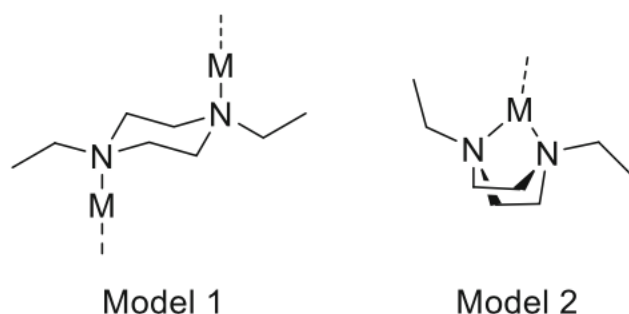


Figure 1: Binding modes for piperazine in the chair (1) and boat (2) conformations

In addition to MOFs, chitosan derivatives containing the piperazine moiety have been complexed to a variety of metal ions to create biodegradable polymers¹⁰. Piperazine polymers have also been shown to exhibit antimicrobial properties when complexed with antimicrobial metals¹¹. Piperazine is biocompatible and stable, making it a strong candidate for use in the development of biomedical scaffolds. Given this information alongside its unique metal binding ability, piperazine is a useful constituent to have in a metallopolymer. If an external stimulus¹² can be utilized to change the environment of the crosslinked metal coordination environment of the scaffold, a degrade-on-demand polymer could be designed and fabricated. The degradation properties of this polymer would introduce a new element to tissue engineering studies and other applications.

One potential avenue of production for metallopolymer scaffolds is the technique of electrospinning. Electrospinning can be used to produce nanofiber scaffolds closely resembling native tissue, making them good contenders for biomedical applications¹³. The mats produced mimic the extracellular matrix and

allow for circulation of oxygen and nutrients, making them particularly useful in tissue engineering. Tissue engineering utilizes scaffolds to contribute an environment for growing cells or tissues to successfully develop into tissues or organs, respectively¹⁴. Degradable polymers are especially desirable in tissue engineering applications due to their chemical properties closely resembling those of many human tissues¹⁵.

The goal of this project was to synthesize a degradable metallopolymer suitable for the previously mentioned applications. A class of thermoplastic piperazine-based polyesters chain extended with urethane linkages was synthesized and characterized. Metal coordination was also performed with the produced polymers and were also characterized. The stability of the non-metal and metal-containing polymers was assessed to investigate their suitability as a material for bioengineering applications.

2 | Methodology

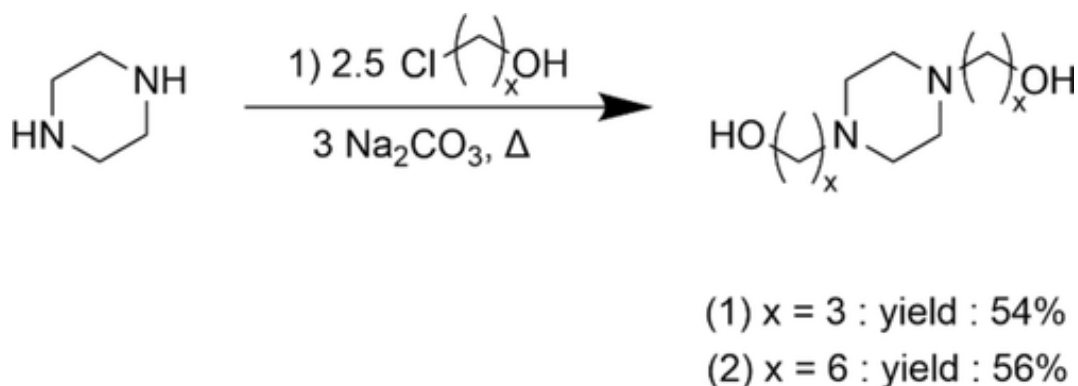
The synthesis aspect of this project was conducted in four steps: synthesis of diols, bulk condensation to generate polymers, chain extension to enlarge the polymers, and metal coordination.

2.1.1 Synthesis of 3,3'-(piperazine-1,4-bis(propan-1-ol))

A one-step synthesis previously reported by Abdelsayed et al¹⁶ was performed to produce compound **1**, 3,3'-(piperazine-1,4-bis(propan-1-ol)). Piperazine (15 g, 174 mmol) was dissolved in 250 mL of absolute ethanol in a single neck 1 L round bottom flask with a magnetic stir bar. Sodium carbonate (55 g, 552 mmol) was added to the flask as a solid and was suspended in the reaction. 3-chloro-1-propanol (41 g, 435 mmol) was added to the flask, and the reaction mixture was heated to reflux for 24 h. The reaction was cooled to room temperature, then the sodium carbonate was removed via vacuum filtration and the ethanol was removed via rotary evaporation. The resulting solid was recrystallized from hot methanol. The white recrystallized solid was then collected via suction filtration and washed with ice cold methanol. The yield of this reaction was 56%, which aligns with the previously reported synthesis' results.

2.1.2 Synthesis of 6,6'-(piperazine-1,4-bis(hexan-1-ol))

The synthesis procedure for compound **2**, 6,6'-(piperazine-1,4-bis(hexan-1-ol)), was identical to that in **1.1**, except the 3-chloro-1-propanol was replaced with 6-chloro-1-hexanol (59 g, 435 mmol). A white powder solid was obtained upon crystallization, as in **1.1**. The yield of this reaction was 53%, again aligning with the previously reported synthesis. The reaction and structures of 3,3'-(piperazine-1,4-bis(propan-1-ol)) and 6,6'-(piperazine-1,4-bis(hexan-1-ol)) are reported in Scheme 1.



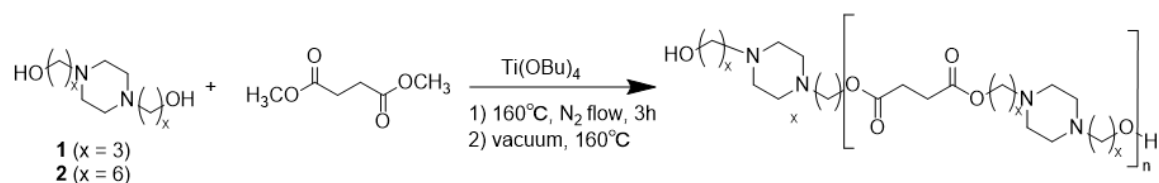
Scheme 1: Structures of 3,3'-(piperazine-1,4-bis(propan-1-ol)) and 6,6'-(piperazine-1,4-bis(hexan-1-ol))

2.2.1 Condensation of piperazine diols with dimethyl succinate

Piperazine diol (**1.1** or **1.2**; 1.2 molar equivalent) and 1 molar equivalent of dimethyl succinate were condensed using a two-step procedure similar to one published by Soccio et al^{17a}. The bulk condensation reactions performed in this step yielded Poly(propyl piperazine succinate) diol (PPPS-OL) from **1.1** and Poly(hexyl piperazine succinate) diol (PHPS-OL) from **1.2**. This step served to produce a starting polymer to work with, containing the useful piperazine moiety.

A dry two neck flask containing a magnetic stir bar was purged with dry nitrogen through a dean stark trap for 30 minutes to eliminate water vapor and oxygen from the reaction vessel. Bis piperazine diol (**1.1** or **1.2**) and dimethyl succinate were added to the purged flask in a 1.65:1 molar ratio. The flask was then heated to 160 °C in a sand bath. The result was a homogeneous colorless molten solution. Once molten, Ti(IV) tetrabutoxide (0.0003 molar equivalents) was added air-free via a syringe. The methanol produced by the resulting reaction was collected in the dean

stark trap. The reaction was allowed to occur for 3 h under positive nitrogen flow. A vacuum was then applied (2 mbar) to the reaction flask and the reaction was held at 160 °C for 1 h. The reaction was then allowed to cool to room temperature. Once cooled, the product was precipitated using a chloroform/acetonitrile solution at -4 °C. Suction filtration was then used to isolate the polymer from the solution. The isolate was washed with acetonitrile and dried in vacuo for 24 h. The reaction scheme for the polymerization is shown in Scheme 2.



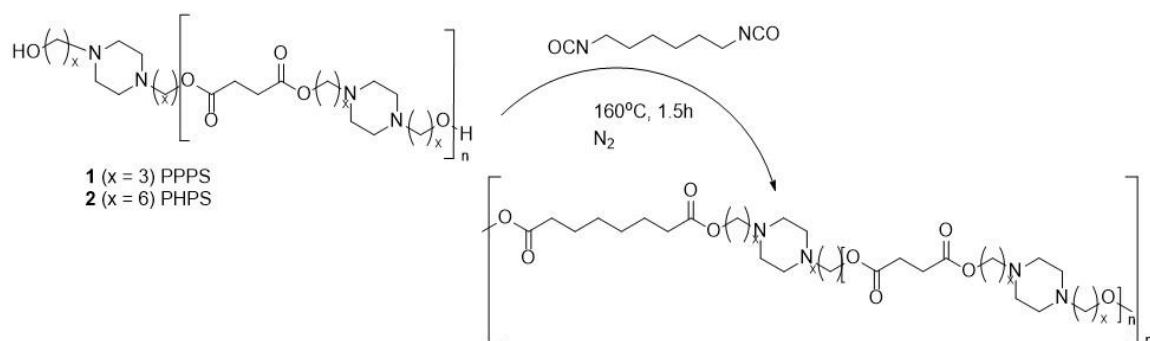
Scheme 2: Polymerization of compounds 1 or 2 with dimethyl succinate

2.3.1 Chain extension of the polyester diols with hexamethylene diisocyanate

Chain extension of PPPS-OL and PHPS-OL was performed similarly to a published procedure^{17b} to enlarge the polymer and promote coordination and entanglement in future steps. A reactor with an overhead stirrer was placed in a 120 °C oven for at least 2 hours to ensure dryness. PPPS-OL or PHPS-OL (30 g, 1 molar equivalent) was added to the dry reactor and was purged with dry nitrogen for 30 min. The reaction was then heated to 130 °C using a silicone oil bath. Once melted, hexamethylene diisocyanate (1.1 molar equivalent) was added to the reaction vessel

air-free via syringe and the reaction was heated at 130 °C for 1 h. The reaction was cooled to room temperature and the white solid product was dissolved in chloroform and precipitated with acetonitrile. The precipitated mixture was cooled at -4 °C overnight. The solid was then collected via vacuum filtration, washed three times with cold acetonitrile, and placed under vacuum until dry.

If this reaction was performed in the presence of oxygen or above 170 °C the polymer rapidly degraded into a dark brown viscous liquid. The reaction was not performed above 130 °C and extensive drying and purging was utilized for this reason. The reaction scheme for the chain extended PPPS-OL, or PPPS-C, and chain extended PHPS-OL, or PHPS-C, is shown in Scheme 3.



Scheme 3: Chain extension of PPPS-OL or PHPS-OL with hexamethylene diisocyanate

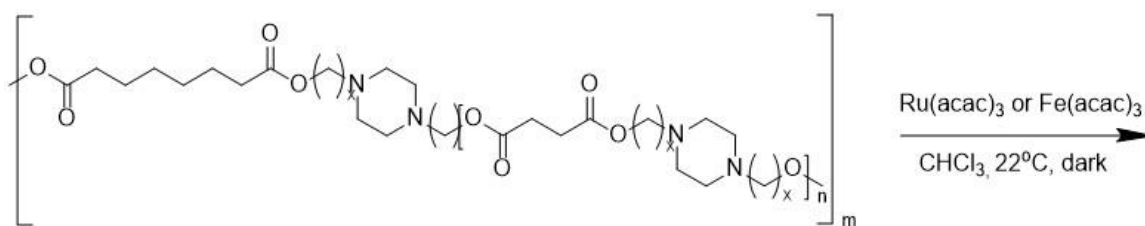
2.4.1 Coordination of Fe(III) into chain extended polypiperazine polyesters

PPPS-C or PHPS-C (1 molar equivalent) were dissolved in 50 mL of dry chloroform and reacted with excess (6 molar equivalents) of Fe(III) acetylacetonate at

room temperature in the absence of light. The reaction mixture was stirred for 48 h, and then the 75% of the chloroform was removed via rotary evaporation at room temperature. Temperature was not increased during rotary evaporation to avoid degradation of the polymer and ensure that the metal would successfully coordinate to the polymer. The remaining solution was precipitated using acetonitrile and cooled overnight at -4 °C. The solid was then isolated using vacuum filtration, and washed with acetonitrile until the washes came out colorless. The resultant metallopolymers, PPPS-C-Fe and PHPS-C-Fe were a dark orange solid and a light orange powder, respectively. The reaction yield was typically around 99%.

2.4.2 Coordination of Ru(III) into chain extended polypiperazine polyesters

The synthesis procedure for PPPS-C-Ru and PHPS-C-Ru was identical to that in **4.1**, except the Fe(III) acetylacetonate was replaced with Ru(III) acetylacetonate. PPPS-C-Ru was a dark red solid and PHPS-C-Ru was a light pink powder. As in **4.1**, the typical reaction yield was around 99%. The metalation reaction scheme is shown in Scheme 4.



Scheme 4: Metalation of chain extended Poly(piperazine succinate) diols with either Fe(III) or Ru(III)

2.5.1 Degradation of polymers with and without metal ions

0.2-0.3 g of each polymer (PPPS-C, PHPS-C, PPPS-C-Fe, PHPS-C-Fe, PPPS-C-Ru, and PHPS-C-Ru) was melted at 90 °C in glass vials to create a 1-2 mm polymer coating. The coating was cooled at room temperature until solidified, and then 4.0 mL of phosphate buffered saline (PBS) and a magnetic stir bar were added to the vial. Periodically, small aliquots of the reaction mixture were removed to test the progress of the reaction. Each aliquot was syringe filtered (0.2 μm PES) and injected in an Agilent 1260 liquid chromatography system with refractive index detector and column oven. The separation was performed using a H-Hiplex column (4.6 x 250 mm, Agilent) with a 50 mM H₂SO₄ mobile phase (0.5 mL/min flow rate) at 60 °C. The concentration of succinate in the reaction was calibrated using external standards between 1-20 mM sodium succinate in PBS. Each degradation experiment was performed twice at either 25 °C or 37 °C, and the average values were found.

2.6.1 Electrospinning of PHPS-C

Electrospinning was performed to exemplify a possible pathway to developing bioengineering scaffolds with the synthesized polymers. PHPS-C was chosen for this experimentation due to its ease to work with. It was a fine white powder, whereas PPS-C tended to be gooey and a bit difficult to work with. A 70/30 solution of PLA/PHPS-C was made at a 12% concentration in an 80/20 chloroform/DMSO solvent system. A 1 mL plastic syringe was loaded with 1 mL of the polymer mixture, and a 21-gauge needle was attached to the syringe. A 10inx10in sheet of non-stick aluminum foil was clipped to an upright stand and placed in front of the needle to act as the collector. The collector was grounded and placed 5 cm from the needle tip. A syringe pump was used to eject the polymer solution at a rate of 1 mL/hr and a voltage of 8.0 kV was applied to the needle tip. Collection took place for approximately 30 minutes, until a white film was visible on the collector.

3 | Results and Data Analysis

Characterization of the poly(alkylpiperazine succinate) diols and chain extended poly(alkylpiperazine succinate) diols was accomplished through HNMR, CNMR, IR, and GPC. ¹H NMR and GPC results were utilized to determine approximate molecular weight values for each polymer. The metal coordination events were confirmed via GPC and UV-vis spectroscopy. Thermal stability of the metallopolymers was investigated. Finally, degradation experiments were performed

to assess the difference in degradation properties between the non-metal and metal-containing polymers.

3.1 Synthesis and characterization of poly(alkylpiperazine succinate) diols

3.1.1 Synthetic methods for PPPS-OL and PHPS-OL

The piperazine-containing polyesters were synthesized via the direct melt condensation of bis alkyl piperazine diols. These diols, which had alkyl chain lengths of either propyl (**1**) or hexyl (**2**), were synthesized using a slightly modified version of a previously published procedure (**Scheme 1**) for **1**¹⁶. After recrystallization from hot methanol, white solids were obtained for both compounds **1** and **2**, with a yield of approximately 50% (**Scheme 1**). The low yield is in line with prior findings for compound **1** and **2**, likely due to the high solubility of the final diol product in water, which makes it challenging to separate from the excess sodium carbonate used in the reaction.

The two diols produced in **Scheme 1** were then utilized in condensation reactions with dimethyl succinate to produce piperazine-containing polymers. The condensation of each diol with dimethyl succinate was performed in slight molar excess (1:2:1) of the diol via a direct melt polymerization to yield poly(alkyl piperazine succinate) diols, PPPS-OL and PHPS-OL (**Scheme 2**). This procedure resembled a previous two-stage direct melt polymerization method using alkyl diols

with succinate^{17b,18}. The two polymer variations were chosen to investigate the effect of chain length (propyl or hexyl) on the distance between interchain linkages with metalation. Upon purification, PHPS-OL was a white solid which was easily precipitated using a chloroform/acetonitrile mixture. PPS-OL, on the other hand, was a viscous, opaque oil which required multiple filtrations with 0.2 μm PVDF membranes to isolate.

3.1.2 NMR spectroscopy of PPS-OL and PHPS-OL

NMR data was collected to determine if the desired products, PPS-OL and PHPS-OL, had been successfully synthesized. The ^1H NMR data is shown in **Figure 2**. Some key resonances were identified to indicate the success. The terminal alcohol groups on the diols (g) are indicated by the peak at 5.0 ppm, the methylene groups adjacent to the ester bonds (c) are indicated by the triplet peaks at 4.1 ppm, and the succinate methylene groups (b) are indicated by the singlet peaks between 2.5-2.6 ppm. Another peak around 2.4 ppm (f) is thought to represent the methylene groups in the piperazine ring based on previous NMR studies¹⁹.

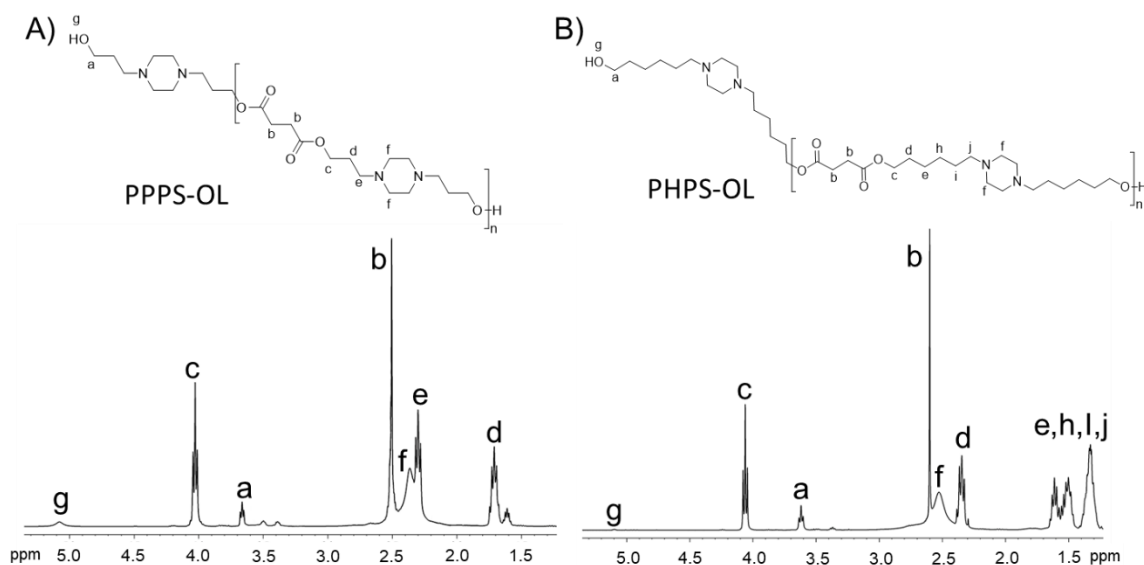


Figure 2: ^1H NMR data for (A) PPPS-OL and (B) PHPS-OL

The ^1H NMR results were also utilized to determine approximate molecular weights of the synthesized polymers, based on a previously published method²⁰. The ratio of integrated intensity between peaks *a* and *c* in the spectra were used to calculate the number of repeating polymer units present, and therefore the weight-average molecular weights for each of the polymers synthesized in this project. These values were compared to the values of molecular weight determined by gas permeation chromatography (GPC) (**Table 1**).

On average, the polymers contained approximately 8-14 repeating units and the molecular weight for PPPS-OL and PHPS-OL typically was in the range of 1800-2700 Da. PPPS-OL tended to have a smaller molecular weight than PHPS-OL. The lower molecular weights are to be expected, as it is difficult to synthesize aliphatic polyesters with molecular weight higher than 30 kDa²¹, and higher temperatures are

normally necessary to obtain higher molecular weight polymers²². When the polymerization reactions were performed at temperatures of 180 °C and above, the reaction mixture began degrading and turned into a viscous brown liquid, so higher temperatures could not be utilized to raise the number of polymeric turnovers. The approach of chain extension allowed for extension of the polymers without degradation from high temperatures.

Polymers	Molecular Weight ($\times 10^3$ g/Mol)			5% weight loss ($^{\circ}\text{C}$) ^F
	M_n^a	M_w^b	PDI M_w/M_n	
PPPS-OL	1.8	2.1	1.2	-
PPPS-C	4.2	7.1	1.7	261
PPPS-C-Ru	4.3	12	2.8	295
PPPS-C-Fe	-	8.2	-	315
PHPS-OL	2.4	3.6	1.5	-
PHPS-C	3.5	6.9	2.0	299
PHPS-C-Ru	3.7	7.6	2.1	302
PHPS-C-Fe	-	7.2	-	319

Table 1: Summary of the molecular weights of the major products from the chain extended polypiperazine polymers and Ru(III) and Fe(III) metallopolymers

3.1.3 GPC results of PPPS-OL and PHPS-OL

Gas permeation chromatography (GPC) was also used to determine the molecular weight values for each of the polymers. A calibration curve was prepared using GPC results from a series of polystyrene standards ranging from 1300-123000 Da. The polystyrene calibration curve was used to calculate the approximate molecular weight of the piperazine polymer based on their GPC retention times. The calculated values are reflected in **Table 1** (M_w).

3.2 Synthesis and characterization of poly(alkylpiperazine succinate) diols

3.2.1 Synthetic methods for PPPS-C and PHPS-C

Chain extension of PPPS-OL and PHPS-OL was performed using hexamethylene diisocyanate (**Scheme 3**). Chain extension allowed for the desired increase in molecular weight while introducing a significant amount of the less hydrolysable urethane bonds²³. The increase in molecular weight can improve material properties and makes the polymer better suited for applications such as electrospinning, as it promotes entanglement and coordination events. After the reaction with hexamethylene diisocyanate took place, PPPS-C and PHPS-C were isolated as solids from precipitation in chloroform/acetonitrile.

3.2.2 IR Spectroscopy of PPPS-C and PHPS-C

Infrared spectroscopy results from the PPPS-OL, PHPS-OL, PPPS-C, and PHPS-C polymers showed key differences indicating that the chain extension had been a success. The comparisons between the poly(alkyl piperazine succinate) diols and their chain extended versions are shown in **Figure 3**. For all four polymers, the ester carbonyl peak was observed at approximately 1720 cm^{-1} . A broad peak at 3300 cm^{-1} was observed in the poly(alkyl piperazine succinate) diols, but not in their chain extended versions. This broad peak is the -OH stretch, and its disappearance in the chain extended polymers was expected as -OH groups in the poly(alkyl piperazine succinate) diols are being replaced in the chain extension reaction. There was also an increase in the peak at 1520 cm^{-1} , which represents that NHCO stretch. This also is expected, as the chain extension is introducing more urethane groups to the polymer chain. Based on the intensity of peaks, it was also deduced that PPPS-C had approximately 30% more urethane compared to PHPS-C.

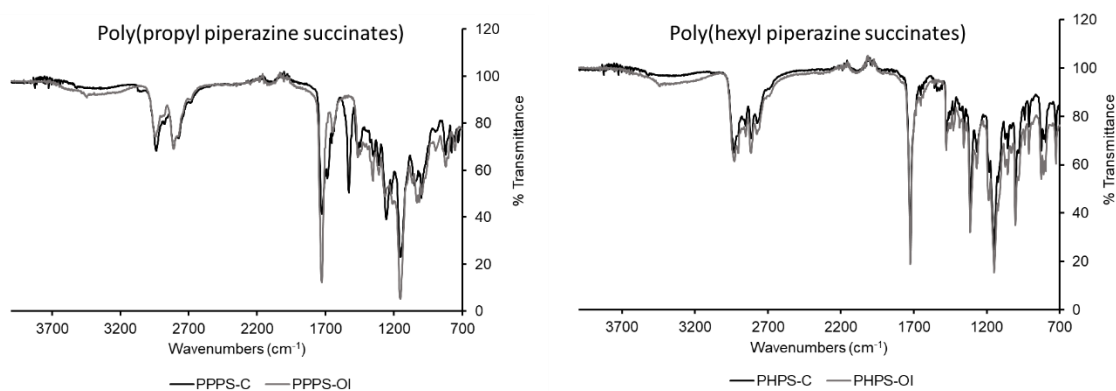


Figure 3: Infrared spectroscopy results for polymers before and after chain extension

3.2.3 GPC results for PPPS-C and PHPS-C

The chain extended polymers, PPPS-C and PHPS-C, were also analyzed using GPC to determine the approximate chain lengths. GPC comparisons between PPPS-OL and PPPS-C, as well as between PHPS-OL and PHPS-C, are shown in **Figure 4**. The calculated molecular weight values are presented in **Table 1**. ^1H NMR was also used to calculate molecular weight values (M_n), as performed with PPPS-OL and PHPS-OL. A significant increase in molecular weight was observed between the poly(alkyl piperazine succinate) polymers and their chain extended versions. This was another indicator that the chain extension had been a success. Notably, the PPPS-OL polymer saw a greater increase in molecular weight as it was converted to PPPS-

C as compared to PHPS-OL to PHPS-C. Regardless, the chain extension was successful in enlarging both polymers.

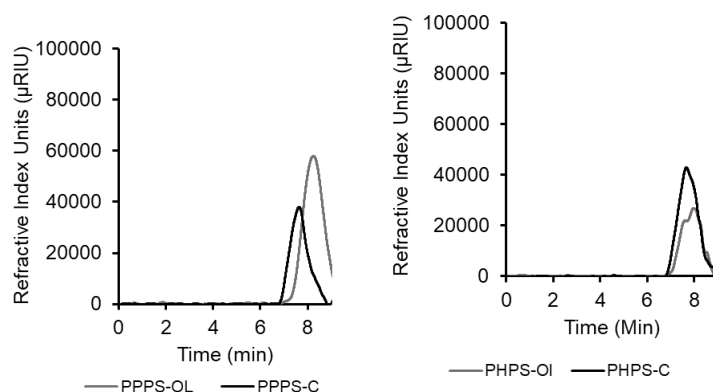


Figure 4: GPC comparisons of polymers before and after chain extension

3.2.4 Thermal analysis of PPPS-C and PHPS-C

Thermogravimetric analysis (TGA) and differential scanning calorimetry (DSC) were utilized to investigate the thermal stability of the chain extended polymers. Thermal properties are significant in electrospinning, as the polymer will be subjected to high electric field that can generate heat, which could potentially degrade the polymer before the mat is obtained. Based on the TGA results, the chain extension step had increased the thermal stability of the polymers. On average, the temperature required to degrade 5% of the polymer weight was increased by 38 °C after chain extension. All the polymers exhibited good thermal stability up to 220 °C.

The DSC results for PPPS-C and PHPS-C are shown in **Figure 5**, alongside their metalated variants. For both PPPS-C and PHPS-C, there was no glass transition state observed. Aside from this, the transitions for the two polymers upon heating were significantly different. PPPS-C displayed its lowest melting point at 47 °C

(**Figure 5A**), whereas PHPS-C exhibited its lowest melting point at 75 °C (**Figure 5B**). Additionally, when PHPS-C was heated, two more endothermic processes were observed at 82 °C and 95 °C (**Figure 5B**). No indications of further melting events at elevated temperatures were observed for either PPPS-C or PHPS-C. The presence of piperazine within the core polymer structure may be responsible²⁴ for the multiple and higher melting phases observed in PHPS-C, as the polymer becomes more disordered. It is also possible that a mesophase transition between a solid and a liquid is occurring.

When PPS-C and PHPS-C were cooled significant differences were observed again. When PPS-C was cooled (**Figure 5C**), significant phase transitions were observed, which confirms the highly disordered nature of this polymer. On the other hand, PHPS-C exhibited a single exothermic transition upon cooling at 62 °C, indicating that it solidified into a single amorphous state (**Figure 5D**). Overall, after multiple heating and cooling cycles, this polymer behaves like a thermoplastic material, exhibiting melting and cold crystallization events but no clear glass transition state. This suggests that these highly aliphatic materials are amorphous.

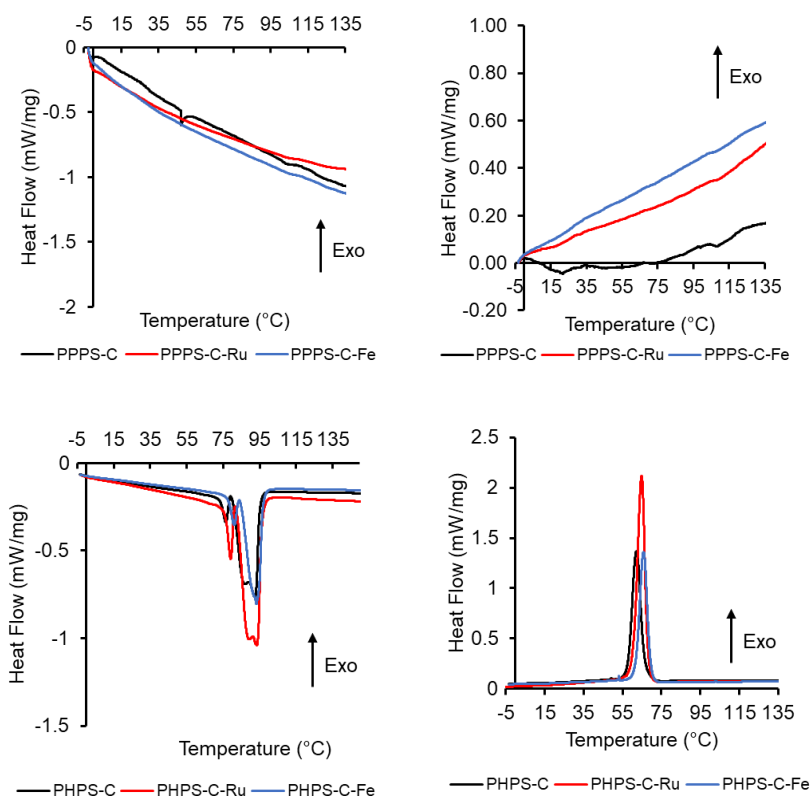


Figure 5: DSC traces of heating from -10 °C to 170 °C (A) PPS-C and (B) PHPS-C at 10 °C/min and the cooling from 170 °C to -10 °C (C) PPS-C and (D) PHPS-C at 10 °C/min with and without Ru(III) or Fe(III)

3.3 Synthesis and characterization of metalated PPS-C and PHPS-C

3.3.1 Synthetic methods for PPS-C-Fe, PPS-C-Ru, PHPS-C-Fe, and PHPS-C-Ru

PPS-C and PHPS-C were metalated in one step at room temperature with either $\text{Ru}(\text{acac})_3$ or $\text{Fe}(\text{acac})_3$ in dry chloroform (**Scheme 4**). This one-step reaction was initially attempted in water, but each experiment resulted in hydrolysis of the polymer, which prevented successful metalation. This experiment was also attempted at higher temperature in chloroform but resulted in degradation of the polymer. Based on this, every step of the experiment was performed at room temperature, including rotary evaporation, to prevent degradation of the polymer and ensure coordination could occur. All metalated products were isolated by precipitation using a chloroform/acetonitrile mixture at $-4\text{ }^\circ\text{C}$. A visible color change was observed upon metalation, giving the initial indication that metal had been coordinated to the polymer.

3.3.2 UV-vis spectroscopy of PPS-C-Fe, PPS-C-Ru, PHPS-C-Fe, and PHPS-C-Ru

Ultraviolet-visible spectroscopy (UV-vis) was performed to investigate whether the metals had been successfully incorporated into the polymers. 3.0 mg/mL

chloroform solutions were made with each of the polymers. The results of the UV-vis spectroscopy are shown in **Figure 6**. For all the metallopolymers, a significant increase in absorbance was observed below 600 nm. This is indicative of the presence of Fe(III) and Ru(III) in the metalated products. For both PPPS-C-Ru and PHPS-C-Ru, two electronic transitions were observed at 495 and 510 nm. For PPPS-C-Fe and PHPS-C-Fe, an increase in absorbance was observed below 500 nm. On its own, UV-vis cannot confirm the coordination of the metals. One possibility is that the metal was adsorbed as an acetylacetonate salt. However, based on ^{13}C NMR results, no resonances consistent with acetylacetonate were present in the polymers, suggesting that this is likely not the case.

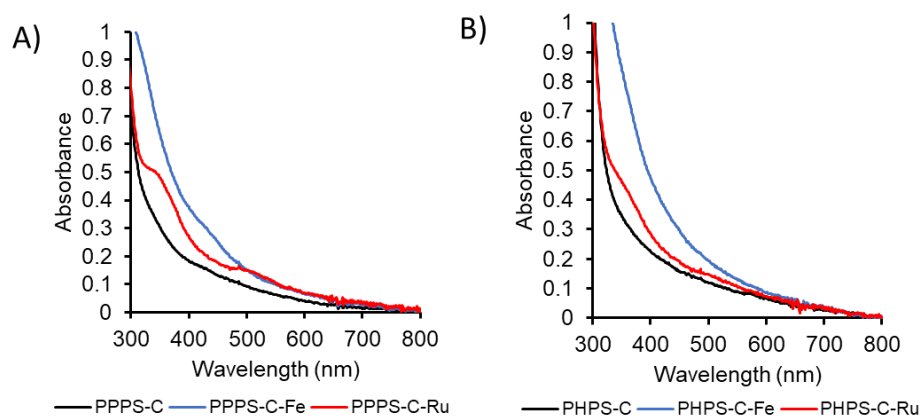


Figure 6: UV-visible spectroscopy data for non-metal and metal-containing polymers

3.3.3 GPC results for PPPS-C-Fe, PPPS-C-Ru, PHPS-C-Fe, and PHPS-C-Ru

GPC was also performed to investigate the coordination events. **Figure 7** compares the GPC data for the unmetalated and metalated polymers. Based on these results, it was found that PPPS-C and PHPS-C had similar molecular weight ranges to their metalated counterparts. This finding indicates that at best, only one metal was coordinated to each piperazine ring. Crosslinking would have resulted in higher overall polymer sizes, which was not observed. There were, however, multiple small peaks eluted before the largest peaks, indicating that some metal crosslinking had occurred. Metallopolymers that eluted at these smaller retention times had much larger molecular weight values but did not greatly contribute to the average molecular weight values.

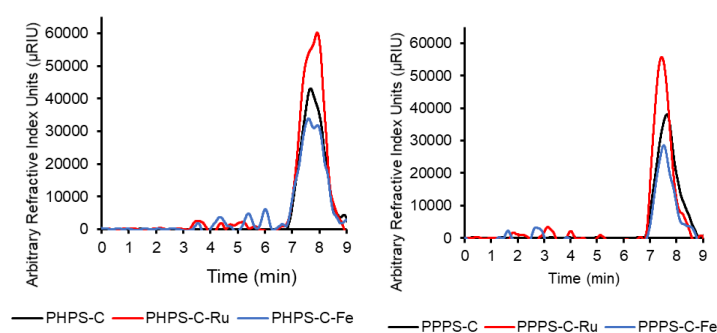


Figure 7: GPC data for non-metal and metal-containing polymers

3.3.4 Thermal analysis of PPPS-C-Fe, PPPS-C-Ru, PHPS-C-Fe, and PHPS-C-Ru

TGA was performed on all metallopolymers. The metallopolymers of both PPPS-C and PHPS-C showed the highest 5% weight loss temperature at an average temperature of 316 °C. This indicates that the coordination of Fe(III) or Ru(III) increased the thermal stability of the chain-extended polymers. All weight losses were two steps if metal was present. Only metalation of PPPS-C with Fe(III) or Ru(III) increased the lower temperature thermal degradation by 52°C. Based on the TGA comparisons, PPPS-C was significantly stabilized thermally through metalation, while the thermal characteristics of PHPS-C metallopolymers remained essentially unchanged.

DSC was also performed on all metallopolymers, and the results are shown in **Figure 5**. The same experimental conditions were used as for the unmetalated polymers. For PPPS-C, there was no distinctive melting or glass transition states with either metal in the heating or cooling experiments. These results suggest that the polymer did not become more crystalline through coordination with the metal centers and are consistent with the GPC data showing that the bulk of the polymer did not undergo crosslinking. For PHPS-C, the Fe(III) polymer showed an increase in melting temperature and a higher temperature solidification transition was observed. These, however, were very small increases. Overall, these results suggest that

crosslinking was not occurring in a large fraction of the metallopolymers, but it was observed that PPPS-C had greater thermal stability upon metalation.

3.4 Investigation of the hydrolysis rates of non-metal and metal-containing polymers

The coordination of metals into polymeric materials can either have a stabilizing or destabilizing effect. Stabilization emerges from cross-linking between polymer strands, and destabilization arises from the reaction of a coordinated metal center with the polymer itself. Maintaining a balance between a polymer material's stability and its eventual degradability rate is a challenge that is still generally unmet. Overall, these poly(alkylpiperazine polymers) present a unique opportunity since introducing a catalytic hydrolytic metal center into a polyester should increase the rate of hydrolysis over time.

Hydrolytic activity of the unmetalated polymers was compared to that of the metallopolymers and is shown in **Figure 8**. Experiments were done at 25 °C and 37 °C in the absence of light. Hydrolysis at 37 °C is of particular interest because it correlates to the desired temperature for mammalian cell studies and future bioengineering applications. HPLC was used to analyze the concentration of succinate in solution over time as the polymer hydrolyzed.

At 25 °C, the unmetalated polymers hydrolyzed the least over 15 days. The metallopolymers hydrolyzed to a greater extent and the rate of succinate release was

increased. Based on the total mass of the polymer coating in the experiment, <5% of the polymer was hydrolyzed without metal present, and approximately 5-20% was hydrolyzed with either metal present.

At 37 °C, the hydrolysis of all metallopolymers was 10 times faster than that of the unmetalated polymers under the same conditions. PPPS-C-Fe has the greatest extent of hydrolysis, reaching 80% over 15 days. Fe(III) polymers hydrolyzed significantly faster than Ru(III) polymers. These results suggest that Ru(III) would be a more stable choice for scaffolding applications, but Fe(III) would be the optimal choice in terms of degradability.

Overall, these results demonstrate that the inclusion of metals in the polymer backbone increases the rate of hydrolysis of the polymers. The slow self-catalytic properties of these metal-containing poly(alkyl piperazine polyesters) presents an approach to catalyzing the hydrolysis of a polymer. By incorporating the piperazine moiety into the polymer backbone, this project created a self-hydrolytic metal activated degradation mechanism to this class of polymers.

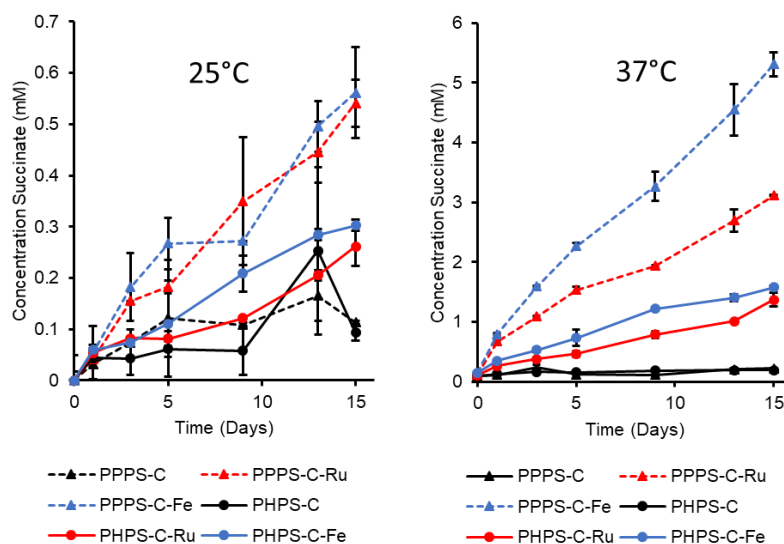


Figure 8: Comparison of hydrolysis for non-metal and metal-containing polymers

3.5 PLA-Polypiperazine Electrospun Mats

Nanofibers were successfully produced from the electrospinning experimentation. A scanning electron microscope was used to image the collected fibers and determine approximate fiber diameter. The images are shown in **Figure 9** at both 1350x and 28500x zoom. Qualitatively, the fibers were determined to be approximately 500 nm in diameter. Future work could look into increasing the ratio of PHPS to PLA in solution and looking into the electrospinnability of PHPS-C-Ru and other synthesized compounds. Overall, this is good evidence that electrospinning could be used to produce bioengineering scaffolds of these polymers for various applications.

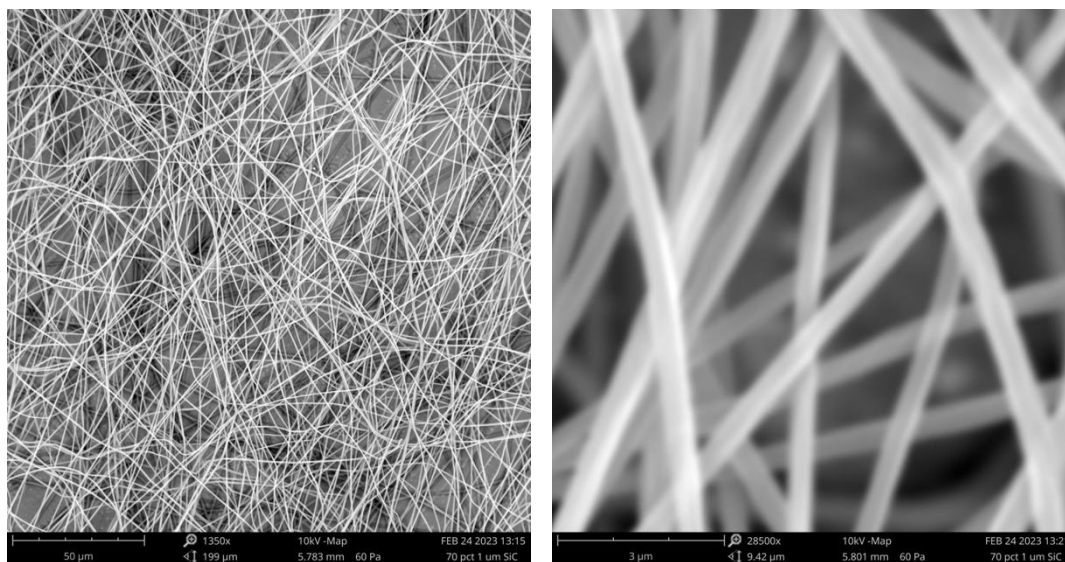


Figure 9: Scanning electron microscope images for PLA/PHPS fibers at (A) 1350x and (B) 28500x

4 | Discussion and Conclusions

This project represents the first reported synthesis and characterization of an aliphatic polypiperazine polyester with urethane chain extension. The polymers were successfully metalated with either Fe(III) or Ru(III) under mild conditions. The hydrolysis experimentation demonstrated that introducing metals into the polymer network results in increased hydrolysis. Electrospinning of PHPS-C was performed and was successful, indicating that electrospinning could potentially be used as a method to produce scaffolds of the synthesized materials. If the original condensation reaction could be optimized, or more metal crosslinking could be induced, then these polymers would be suitable for more biomedical applications.

5 | References

- [1] a A. S. Abd-El-Aziz, A. A. Abdelghani, A. K. Mishra, *J. Inorg. Organomet. Polym. Mater.* **2020**, *30*, 3; b Z. L. Sun, J. H. Li, W. Y. Wong, *Macromol. Chem. Phys.* **2020**, *30*, 3.
- [2] H.Lian,X.Z.Cheng,H.T.Hao,J.B.Han,M.T.Lau,Z.K.Li, Z. Zhou, Q. C. Dong, W. Y. Wong, *Chem. Soc. Rev.* **2022**, *51*, 1926.
- [3] a A. Kumar, S. Bawa, K. Ganorkar, S. K. Ghosh, A. Bandyopadhyay, *Polym. Chem.* **2020**, *11*, 6579; b M. T. Nguyen, R. A. Jones, B. J. Holliday, *Coord. Chem. Rev.* **2018**, *377*, 237.
- [4] L. H. Lai, D. Luo, T. Liu, W. J. Zheng, T. F. Chen, D. Li, *ChemistryOpen* **2019**, *8*, 434.
- [5] a E. Vorobyeva, F. Lissel, M. Salanne, M. R. Lukatskaya, *ACS Nano* **2021**, *15*, 15422; b H. Z. Gao, R. N. Yu, Z. W. Ma, Y. S. Gong, B. A. Zhao, Q. L. Lv, Z. A. Tan, *J. Polym. Sci.* **2022**, *60*, 865.
- [6] R. Kant, S. Maji, *Dalton Trans.* **2021**, *50*, 785.
- [7] M. Shaquiquzzaman, G. Verma, A. Marella, M. Akhter, W. Akhtar, M. F. Khan, S. Tasneem, M. M. Alam, *Eur. J. Med. Chem.* **2015**, *102*, 487.
- [8] M. Ding, W. Liu, R. Gref, *Adv. Drug Deliv. Rev.* **2022**, *190*, 114496.
- [9] a Q. He, H. Zhao, Z. Teng, Y. Wang, M. Li, M. R. Hoffmann, *Chemosphere* **2022**, *303*, 134987; b J. Tao, R. Tan, L. Xu, J. Zhou, Z. Yao, Y. Lei, P. Chen, Z. Li, J. Z. Ou, *Small Methods* **2022**, *6*, 2200429.
- [10] K. R. Krishnapriya, M. Kandaswamy, *Carbohydr. Res.* **2010**, *345*, 2013.
- [11] C. S. Karthik, H. M. Manukumar, A. P. Ananda, S. Nagashree, K. P. Rakesh, L. Mallesha, H.-L. Qin, S. Umesha, P. Mallu, N. B. Krishnamurthy, *Int. J. Biol. Macromol.* **2018**, *108*, 489.
- [12] a R. Weinstain, T. Slanina, D. Kand, P. Klan, *Chem. Rev.* **2020**, *120*, 13135; b W. Zhao, Y. M. Zhao, Q. F. Wang, T. Q. Liu, J. J. Sun, R. Zhang, *Small* **2019**, *15*, 1903060.

- [13] M. Rahmati, D. K. Mills, A. M. Urbanska, M. R. Saeb, J. R. Venugopal, S. Ramakrishna, M. Mozafari, *Prog. Mater. Sci* **2021**, 117, 100721.
- [14] I. Jun, H. Han, J. R. Edwards, H. Jeon, *Int. J. Mol. Sci.* **2018**, 19, 745.
- [15] A. Kirillove, T. R. Yeazel, D. Asheghali, S. R. Petersen, S. Dort, K. Gall, M. L. Becker, *Chem. Rev.*, **2021**, 121, 18.
- [16] S. Abdelsayed, N. T. H. Duong, C. Bureau, P. P. Michel, E. C. Hirsch, J. M. E. Chahine, N. Serradji, *BioMetals* 2015, 28, 1043.
- [17] a M. Soccio, N. Lotti, L. Finelli, M. Gazzano, A. Munari, *J. Polym. Sci. Part B Polym. Phys.* 2008, 46, 170; b G. Guidotti, M. Soccio, V. Siracusa, M. Gazzano, E. Salatelli, A. Munari, N. Lotti, *Polymers* 2017, 9, 724.
- [18] L. C. Zheng, C. C. Li, W. G. Huang, X. Huang, D. Zhang, G. H. Guan, Y. N. Xiao, D. J. Wang, *Polym. Adv. Technol.* 2011, 22, 279.
- [19] B. Qin, J. Lin, Z. Lin, Y. Xue, H. Ren, *Spectrochim. Acta, Part A* 2005, 61, 665.
- [20] J. U. Izunobi, C. L. Higginbotham, *J. Chem. Educ.* 2011, 88, 1098.
- [21] M. Sokolsky-Papkov, R. Langer, A. J. Domb, *Polym. Adv. Technol.* 2011, 22, 502.
- [22] C. Zhu, Z. Zhang, Q. Liu, Z. Wang, J. Jin, *J. Appl. Polym. Sci.* 2003, 90, 982.
- [23] K. Matyjaszewski, M. Moller, in *Polymer Science: A Comprehensive Reference* (Eds: T. Loontjens, E. Goethals), Elsevier Science, Amsterdam 2012.
- [24] M. D. Jalageri, Y. M. Puttaiahgowda, A. M. Parambil, A. Kulal, *J. Appl. Polym. Sci.* 2019, 136, 47521.